Stepwise excitation and level-crossing spectroscopy of the triplet D states of helium-4†

Andrew C. Tam
Columbia Radiation Laboratory, Department of Physics, Columbia University, New York, New York 10027
(Received 9 April 1975)

The fine-structure intervals of the lowest two triplet D states of ^{4}He have been obtained by a new method: Ground-state atoms are excited by a discharge to the triplet metastable state, which then undergoes a two-step optical excitation to the triplet D states, where level-crossing measurements are made. The experimental results for $^3D_1$-$^3D_3$ (MHz) are 1400.67 ± 0.29 and 591.25 ± 0.14 for the $3\,^3D$ and $4\,^3D$ states, respectively; for $^3D_2$-$^3D_3$ (MHz) they are 75.97 ± 0.23 and 36.15 ± 0.24 for $3\,^3D$ and $4\,^3D$. These values are much more precise than the previously available data, obtained by optical, particle-bombardment level crossing, or beam-foil quantum-beat spectroscopy, and are consistent with the previous data except for one case, where a previous measurement of $3\,^3D_2$-$3\,^3D_3$ by electron bombardment level-crossing spectroscopy is believed to be in error. These new experimental values for the fine structures of the triplet D states of ^{4}He clearly indicate the inadequateness of existing theoretical calculations of these fine structures.

I. INTRODUCTION

The experimental determination of the fine structure of the triplet D states of ^{4}He (or an isoelectronic ion) is of very special interest in atomic physics, because it provides a critical test for a calculation on the L-related properties of a two-electron system, where L is the total orbital angular momentum. For example, two recent calculations[1,2] on the important subject of singlet-triplet mixing in helium predict the following: (i) mixing increases from zero for S states to near complete for F or higher-L states; and (ii) mixing decreases as the principal quantum number n increases. However, the values for the mixing coefficients given by these two calculations[1,2] differ significantly (by up to a factor of 2). Furthermore, the theoretical predictions seem to contradict some rather qualitative experimental findings: experiments[3] on proton excitation of helium seems to indicate much larger singlet-triplet mixing in $3D$ than predicted, while experiments[4] on electron excitation of helium seem to indicate that mixing increases as n increases for the F states. Thus, there are serious doubts as to the validity of the calculations on the singlet-triplet mixing in D states, and other states, in helium. An accurate experimental determination of the fine structure of the D states provides a critical test of any calculation on mixing coefficients and fine-structure intervals (these two quantities come from the same set of integrals).

The previous measurements of the $n\,^3D$ fine structure all employ direct nonoptical production of the state from the ground state; the methods include optical spectroscopy,[5] electron-bombardment level-crossing spectroscopy,[6] ion-bombardment level-crossing spectroscopy,[7,8] and beam-foil quantum-beat spectroscopy.[9] All previously available experimental data on the lowest two ^3D states are listed in Table I. Accuracies obtained are about 1% or worse, except in one case, where Kaul,[7] using ion-bombardment level-crossing spectroscopy, obtained the $3\,^3D_1$-$3\,^3D_2$ intervals as 1327.2 ± 1.1 MHz. The previous measurements of the fine structure all suffer from some accuracy-limiting drawbacks: Optical spectroscopy obviously suffers from the large Doppler broadening of helium. Electron-bombardment level-crossing spectroscopy suffers mainly from the serious curvature of the electron beam, and the curvature changes as the applied magnetic field changes. This effect tends to cause a systematic error in the measurements of the fine or hyperfine structures, which may explain why the fine structures of $4\,^3P$ and $5\,^3P$ states of ^{4}He obtained by this method are significantly less than those obtained by microwave-optical techniques.[10] Ion-bombardment level-crossing spectroscopy suffers from the fact that ions are rather inefficient in producing a triplet D state (with an alignment) from the singlet ground state, and hence a long integration time is needed. Beam-foil quantum-beam spectroscopy[9,11] apparently lacks the accuracy that level-crossing spectroscopy or optical double-resonance spectroscopy are capable of, perhaps because it is not easy to make precise measurements of the modulation of the decaying fluorescence as a function of position or time.

In the present experiment, a new method involving a three-step excitation to a ^3D state has been used to obtain fine-structure intervals in the ^3D state. Fluorescence from $3\,^3D$, $4\,^3D$, or $5\,^3D$ at 5876, 4472, or 4026Å, respectively, was observed. All the $\Delta m = 2$ level-crossing signals in $3\,^3D$ and $4\,^3D$ states have been observed. Attempts to observe level crossings in higher ^3D states have not been successful yet, due to too much

stray light being detected with the present apparatus. For the two states studied, the fine-structure intervals are obtained with much improved accuracies.

II. THEORY OF THE FINE STRUCTURES OF ^{4}He

The Breit Hamiltonian H_B describes the fine-structure interaction and singlet-triplet mixing (to order α^2) in a heliumlike ion of nuclear charge Z, and is given by the following, in atomic units[12]:

$$H_B = H_{SO} + H_{SS} , \tag{1}$$

where

$$H_{SO} = H_{SO}^n + H_{SO}^e , \tag{2}$$

with

$$H_{SO}^n = \tfrac{1}{2}\alpha^2 Z(\vec{l}_1\cdot\vec{s}_1/r_1^3 + \vec{l}_2\cdot\vec{s}_2/r_2^3) , \tag{3a}$$

$$H_{SO}^e = -\tfrac{1}{2}\alpha^2(\vec{l}_{12}\cdot\vec{s}_1 + \vec{l}_{21}\cdot\vec{s}_2)/r_{12}^3 - \alpha^2(\vec{l}_{21}\cdot\vec{s}_1 + \vec{l}_{12}\cdot\vec{s}_2)/r_{12}^3 , \tag{3b}$$

and

$$H_{SS} = (\alpha^2/r_{12}^5)[r_{12}^2\vec{s}_1\cdot\vec{s}_2 - 3(\vec{s}_1\cdot\vec{r}_{12})(\vec{s}_2\cdot\vec{r}_{12})] , \tag{4}$$

where $\vec{r}_{12} = \vec{r}_1 - \vec{r}_2$, $\vec{l}_{12} = \vec{r}_{12}\times\vec{p}_1$, and $\vec{l}_{21} = \vec{r}_{21}\times\vec{p}_2$.

Equation (3a) gives the self-spin-orbit coupling of each electron through the Coulomb field of the nucleus; Eq. (3b) gives the self-spin-orbit coupling of each electron through the Coulomb field of the other electron, together with the mutual spin-orbit coupling between the two electrons. Equation (4) gives the spin-spin interaction between the two electrons. We may note that the complete Breit Hamiltonian contains other terms (like "contact-interaction" terms) which do not affect fine structures or singlet-triplet mixing, and these terms have been omitted.

We shall limit our attention to the case of single-excited electrons only, i.e., with the inner electron in a 1s state, and the outer electron in a nl state. Hence the total electronic orbital angular-momentum L equals l. We shall work with the following four degenerate "basis states" with the same J_z:

$$\begin{aligned} &\varphi_1\text{: singlet state with } J = L ;\\ &\varphi_2\text{: triplet state with } J = L ;\\ &\varphi_3\text{: triplet state with } J = L+1 ;\\ &\varphi_4\text{: triplet state with } J = L-1 . \end{aligned} \tag{5}$$

The matrix elements of $H_B + 1/r_{12}$ with respect to the basis states given by Eq. (5) can be conveniently expressed in terms of a few "reduced" matrix elements, as was done by Araki *et al.*,[13] whose results are given in Eq. (6):

$$1/r_{12} + H_B = \begin{bmatrix} K & -2[L(L+1)]^{1/2}\zeta' & 0 & 0 \\ -2[L(L+1)]^{1/2}\zeta' & -K-2\zeta \\ & -2(2L-1)(2L+3)\eta & 0 & 0 \\ 0 & 0 & -K+2L\zeta \\ & & +2L(2L-1)\eta & 0 \\ 0 & 0 & 0 & -K-2(L+1)\zeta \\ & & & +2(L+1)(2L+3)\eta \end{bmatrix} , \tag{6}$$

where K is the exchange integral, ζ the "reduced" spin-orbit matrix element in the triplet states (or the spin-orbit parameter), η the "reduced" spin-spin matrix element in the triplet state (or the spin-spin parameter), and ζ' the "reduced" spin-orbit matrix element between the singlet and the triplet state (or the mixing parameter).

From Eq. (6), we see that $J = L+1$ or $J = L-1$ states are pure triplet states; however, the $J = L$ eigenstates for nonzero L are mixtures of singlet and triplet states, i.e., the predominantly triplet $J = L$ eigenstate Φ_t (often simply called the triplet $J = L$ state) is given by

$$\Phi_t = (\gamma\varphi_1 + \varphi_2)/(1+\gamma^2)^{1/2} , \tag{7}$$

where γ is the so-called mixing coefficient,[1,14,15] obtainable by diagonalizing Eq. (6). Calculations[1,2] show that in helium, $\gamma \sim 10^{-4}$ for P states, $\sim 10^{-2}$ for D states and ~ 1 for F, G states. If the exchange integral K is much larger than ζ, η, and ζ', then

$$\gamma \approx [L(L+1)]^{1/2}\zeta'/K . \tag{8}$$

The eigenenergies of $1/r_{12} + H_B$ are obtained by the simple diagonalization of the matrix given in Eq. (6). The effect on the eigenenergies, as various parts of the operator $1/r_{12} + H_B$ are introduced, is illustrated schematically in Fig. 1.

The (triplet) fine-structure intervals are[13]

$$\begin{aligned} E(J=L-1) - E(J=L+1) &= 2(2L+1)(-\zeta+3\eta) ,\\ E(J=L) - E(J=L+1) &= 2(L+1)[-\zeta - 3(2L-1)\eta] \\ &\quad - \delta E_{st} , \end{aligned} \tag{9}$$

where δE_{st} is a positive quantity not necessarily small compared with $|\zeta|$ or $|\eta|$, and represents

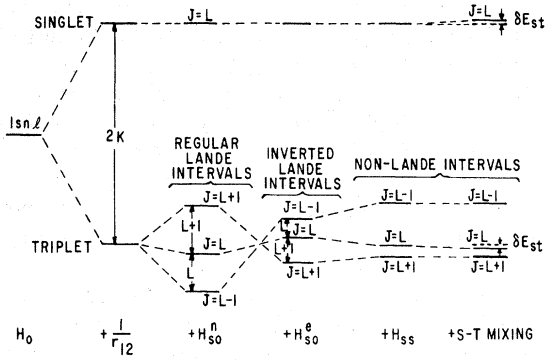

FIG. 1. Effect on the eigenenergies as various parts of the operator $1/r_{12} + H_B$ are introduced.

the "repulsion" between the singlet and the triplet $J = L$ eigenstates due to their mixing. Theoretical results of the fine-structure intervals for the lowest two ^3D states, all calculated according to the above scheme but with various approximations, are listed in Table I.

III. THEORY OF STEPWISE EXCITATION LEVEL-CROSSING SPECTROSCOPY

The theory of the effect on atomic fluorescence due to level crossing[18] for the case of a one-step optical excitation is well established in the literature,[19,20] and is summarized in the Breit-Franken formula.[21] However, for a two-step optical excitation, the fluorescence from the higher excited state m is complicated by the presence of the lower excited state μ, in which optical pumping, level crossing, etc. would cause "interference effects."[22] We shall simply call the fluorescence from the higher excited state m stepwise fluorescence, following the nomenclature of Kibble and Pancharatnam,[22] who first dealt with the theory of stepwise fluorescence in a semiclassical perturbation treatment involving polarizability, for white-light excitation. We shall derive the formula for the stepwise fluorescence in another way, in a density-matrix formalism along the line of Gupta, Chang, and Happer.[23] The sublevels of the ground state, lower excited state, higher excited state, and final state are labeled g, μ or μ', m or m', and n, respectively. The density matrix of the ground state, lower excited state, and higher excited state are denoted by ρ^S, ρ^P, and ρ^D, respectively. At steady state (i.e., rate of change of density matrices being zero) and for white-light excitation, the density matrix of the lower excited state is related to that of the ground state by[23]

TABLE I. Fine-structure intervals of $3\,^3$D and $4\,^3$D states in ^{4}He.

Work	Fine-structure intervals in MHz $3\,^3D_1 - 3\,^3D_3$	$3\,^3D_2 - 3\,^3D_3$	$4\,^3D_1 - 4\,^3D_3$	$4\,^3D_2 - 4\,^3D_3$
Experiment				
Present work	1400.67 ± 0.29	75.97 ± 0.23	591.25 ± 0.14	36.15 ± 0.24
Brochard *et al.*[a]	1448 ± 30	90 ± 24	615 ± 30	54 ± 30
Descoubes[b]		72.5 ± 0.5		35.8 ± 0.4
Buchhaupt[c]		74.6 ± 1.0		35.8 ± 1.0
Kaul[d]	1399.9 ± 1.1			
Berry *et al.*[e]	1420 ± 25	71 ± 2	576 ± 30	40 ± 5
Theory				
Araki[f]	1353	75	567	28.5
Bethe, Salpeter[g]	1390	92.7	587	39.1
Moser *et al.*[h,i]	1409	83.8	598	41.1
Parish, Mires[j]	1473	126	633	60
Van den Eynde *et al.*[h,k]	1414	85.8	600	41.8

[a] Reference 5.
[b] Reference 6.
[c] Reference 8.
[d] Reference 7.
[e] Reference 9.
[f] Reference 16.
[g] Reference 12.
[h] Note: fine structures not explicitly given by these authors, but derived from their work.
[i] Reference 17.
[j] Reference 2.
[k] Reference 1.

$$\rho^{P}_{\mu\mu'} \propto \frac{\langle \mu | \vec{f}\cdot\vec{p}\rho^{S}\vec{p}\cdot\vec{f}^{*} | \mu' \rangle}{\Gamma_{\mu} + i\omega_{\mu\mu'}} , \tag{10}$$

where $\vec{f}$ is the polarization of the first-step excitation light, $\vec{p}$ is the dipole operator, and Γ_{μ} is the reciprocal of the coherence lifetime of the lower excited state. Similarly,

$$\rho^{D}_{mm'} \propto \frac{\langle m | \vec{e}\cdot\vec{p}\rho^{P}\vec{p}\cdot\vec{e}^{*} | m' \rangle}{\Gamma_{m} + i\omega_{mm'}} \tag{11}$$

where $\vec{e}$ is the polarization of the second-step excitation light. The intensity $I(\vec{f}, \vec{e}, \vec{u})$ of the stepwise fluorescence of polarization $\vec{u}$, is given by[23]

$$I(\vec{f}, \vec{e}, \vec{u}) = \mathrm{Tr}(\rho^{D}\mathcal{L}) , \tag{12}$$

where $\mathcal{L}$ is the fluorescence light operator[23]:

$$\mathcal{L} \propto \sum_{n} \vec{u}\cdot\vec{p} | n \rangle\langle n | \vec{p}\cdot\vec{u}^{*} . \tag{13}$$

Thus, the stepwise fluorescence intensity I is given for white-light excitation, in general, by combining Eqs. (10)–(13). If we further assume a totally unpolarized ground state (not optically pumped), i.e., assume

$$\rho^{S} = \frac{1}{N_{g}} \sum_{g} | g \rangle\langle g | , \tag{14}$$

where N_g is the total number of ground-state sublevels, then we can easily see that the stepwise fluorescence would be given by

$$I(\vec{f}, \vec{e}, \vec{u}) = K \sum_{\substack{g\mu\mu' \\ mm'n}} \frac{(u_{nm}e_{m\mu}f_{\mu g})(u_{nm'}e_{m'\mu'}f_{\mu' g})^{*}}{(\Gamma_{\mu} + i\omega_{\mu\mu'})(\Gamma_{m} + i\omega_{mm'})} , \tag{15}$$

where K is a constant, $f = \vec{f}\cdot\vec{p}$, $e = \vec{e}\cdot\vec{p}$, $u = \vec{u}^{*}\cdot\vec{p}$. Equation (15), first derived by Kibble and Pancharatnam by a semiclassical perturbation method, may be called the "extended Breit-Franken formula" for stepwise fluorescence. It is convenient to separate $I(\vec{f}, \vec{e}, \vec{u})$ for an unpolarized ground state and white-light excitation, given by Eq. (15), into four parts, given by imposing different conditions on the sixfold summation: (i) $\mu = \mu'$ and $m = m'$; (ii) $\mu \neq \mu'$ and $m = m'$; (iii) $\mu = \mu'$ and $m \neq m'$; (iv) $\mu \neq \mu'$ and $m \neq m'$. We shall call these parts the decoupling term I_{dec}, the absorption level-crossing term I_{abs}, the conventional level-crossing term I_{con}, and the multiplicative level-crossing term I_{mul}, respectively. The last three names were introduced by Kibble and Pancharatnam.[22] The term I_{dec} is a slow varying function of the magnetic field, and shows no resonance feature since there is no energy denominator. The term I_{abs} describes the effect of level crossing in the lower excited state, where coherence created is partly transformed into populations in the higher excited state. The term I_{con} describes the effect of level crossing in the higher excited state, and this term is almost identical to the Breit-Franken formula except for the presence of "weighing factors" $|f_{\mu g}|^{2}$. The term I_{mul} describes the effect of the overlapping of a level crossing in the lower excited state with a crossing in the higher excited state, when coherence created in the former is partly carried over into coherence in the latter. The various routes in a two-step optical excitation giving rise to the absorption, conventional, and multiplicative level-crossing terms are illustrated in Fig. 2. We may note that at small magnetic field (Hanle-effect region), all three terms I_{abs}, I_{con}, and I_{mul} are nonzero, and analysis is rather complicated. However, at large field (i.e., outside the Hanle-effect region), overlapping of crossings in the lower and higher excited states occur only infrequently, and hence we can usually describe a resonance in the stepwise fluorescence by I_{abs} alone or by I_{con} alone, when crossing occurs only in the lower, or higher, excited states, respectively. We may also note that the complicating effect of optical pumping in the ground state or of resonance light trapping is significant only when overlapping of level-crossing signals occurs; otherwise pure Lorenztian or pure dispersion signals in the stepwise fluorescence could always be obtained for an isolated level crossing (in the upper excited state or in the lower excited state).

IV. ZEEMAN SUBLEVELS OF THE TRIPLET D STATES

The complete Hamiltonian of a helium atom in an external magnetic field $\vec{H}$ is

$$\mathcal{H} = H_{\mathrm{FS}} + [(g_{S} - g_{L})S_{z} + g_{L}m]\mu H , \tag{16}$$

where H_{FS} is the fine-structure Hamiltonian, and m is the total z component (parallel to $\vec{H}$) of angular momentum and is a good quantum number; H_{FS} is diagonal in the (J, m) representation, and for the $^{3}D_{3}$, $^{3}D_{2}$, and $^{3}D_{1}$ eigenstates, the eigen-

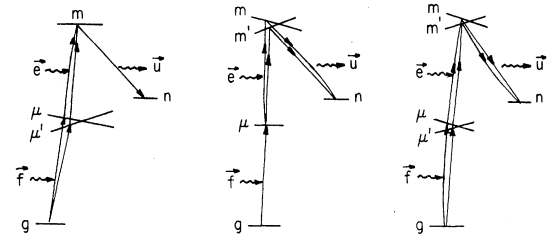

(a) ABSORPTION LEVEL CROSSING (b) CONVENTIONAL LEVEL CROSSING (c) MULTIPLICATIVE LEVEL CROSSING

FIG. 2. Various routes in a two-step optical excitation giving rise to observable level-crossing signals.

values are 0, E_2, and E_1, respectively. (We shall set the zero of the energy scale at E_3.) Note that the $^3D_2$ eigenstate is actually not pure triplet, but has about 1% singlet admixture.[1,2] The "diamagnetic Zeeman interaction"[10,32] has been left out in Eq. (16), since it is estimated as too small to affect our results significantly in our range of magnetic field (up to 600 G).

Near zero field, the Zeeman splittings are characterized by the following g_J values:

$$g_3 = g_L + \tfrac{1}{3}(g_S - g_L)\,, \tag{17}$$

$$g_2 = g_L + \tfrac{1}{6}(g_S - g_L)\alpha_t^2\,, \tag{18}$$

$$g_1 = g_L - \tfrac{1}{2}(g_S - g_L)\,, \tag{19}$$

where α_t is the triplet coefficient in the "triplet" $J=2$ eigenstate, and [see Eq. (7)] is related to the mixing coefficient γ by

$$\alpha_t = (1+\gamma^2)^{-1/2} \approx 1 - \tfrac{1}{2}\gamma^2\,. \tag{20}$$

To compute numerically the Zeeman levels, values for α_t, g_L, g_S are taken as

$$\alpha_t = 0.99995 \pm 0.00005\,, \tag{21a}$$

$$g_L = 0.999867 \pm 0.00001 \text{ (Ref. 24)}\,, \tag{21b}$$

$$g_S = 2.00229 \pm 0.00004 \text{ (Ref. 25)}\,. \tag{21c}$$

The value for the triplet coefficient α_t given in Eq. (21a) is estimated from the calculated singlet-triplet mixing coefficients[1,2] and from the condition $|\alpha_t| \leq 1$. Values for g_L and g_S have been put as those used for ^3P states,[24,25] and the uncertainties given in Eqs. (21b) and (21c) are due to possible relativistic and motional corrections[24] to the g values. The computed results for $3\,^3D$ are shown in Fig. 3 (the present experimental values for E_1 and E_2 are used), where all eight $\Delta m = 2$ level crossings are identified.

It can easily be calculated that the low-field crossings A, B, C, and D are unresolved, while the high-field crossings P, Q, R, and S are all resolved. Accurate experimental determinations of the high-field crossing points (and the over-all low-field crossing signal) would not only yield E_1 and E_2, but also give consistency checks and possibly give indications of the best values for α_t, g_L, and g_S for the state concerned. For the $3\,^3D$ and $4\,^3D$, only one high-field crossing (the Q crossing) of $3\,^3D$ has been studied by ion bombardment,[7] and this Q crossing field has to be combined with the rather uncertain "combined low-field crossing signal"[6] to give the fine-structure intervals of $3\,^3D$. No optical excitation to the ^3D states has ever been attempted, though this method of excitation potentially gives the best accuracy, because photons are not affected by magnetic field, and usually are more efficient in producing coherence than electrons or ions. A major difficulty is that ^3D states are not optically accessible in one step either from the ground state or from a metastable state. This difficulty is overcome in our present experiment.

V. EXPERIMENTAL SETUP

In the present experiment, a ^3D state is produced by two successive optical excitations from the $2\,^3S$ metastable state produced by a low pressure helium discharge. The scheme of this method is illustrated in Fig. 4. Spectroscopy involving a three-step excitation scheme has never been attempted before. The following points seem to be the obvious experimental difficulties.

(i) The metastable state must be created and maintained at a sufficient density in a way that is least affected by a varying magnetic field and produces a minimum of background light.

(ii) A bright, stable, and not self-reversed light source is needed for each optical excitation: 10830 Å for the first-step excitation, and 5876Å ($3\,^3D$) or 4472 Å ($4\,^3D$) for the second-step excitation. Since only the 5876-Å line is within the tuning range of cw dye lasers, good spectral lamps and appropriate focusing devices must be designed.

(iii) Since the fluorescence observed is of the same wavelength as the incident second-step excitation light, the instrumental scattering must be minimized.

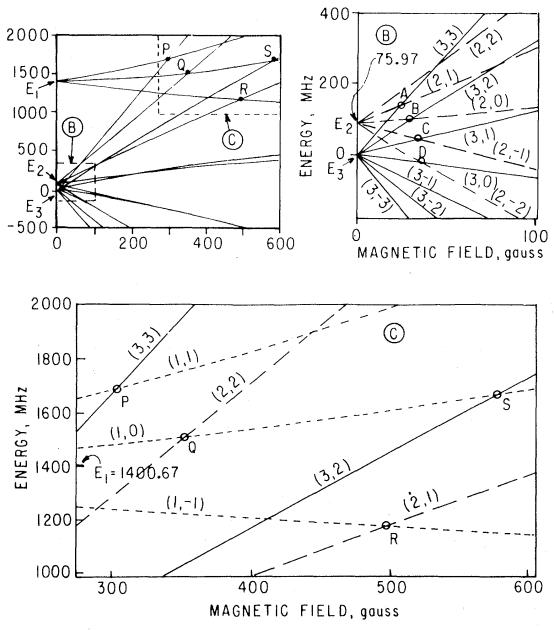

FIG. 3. Zeeman level diagram for the $3\,^3D$ state of ^{4}He.

In our setup, metastable atoms are created in a discharge-absorption cell (Fig. 5), designed to run a stable dc discharge at about 10–50 mA and 30–200 mtorr of helium. At these low pressures, a hot cathode is needed to sustain a quiet and sputtering-free discharge. A flat grid is positioned in the cell as shown in Fig. 5. A voltage of about −10 V with respect to the cathode is applied to this grid to prevent the discharge from extending to the central (observation) region of the cell. Much of the cell surface is painted flat black to minimize instrumental scattering.

The Pyrex discharge-absorption cell has i.d. = 3.75 in. and the separation between windows is 3.5 in. After the cell is fabricated, it is pumped out to better than 10^{-6} torr while baked at 300 °C for one day. The filament is activated, and the pumping and baking is repeated for another day. Then the cell is cooled, is "purged" by a discharge for a few times, and is then filled at the experimental pressure, typically 60 mtorr. The rigorous cleaning procedure for the cell before filling ensures that helium $2\,^3S$ metastable atoms would have little probability of being quenched by impurity atoms. Furthermore, the rather large size of the cell means long diffusion times (~10^{-3} sec) so that a satisfactory metastable density (typically 10^{10} cm^{-3}) can be built up at the center of the cell.

A resonance lamp for the present experiment has the basic geometry of a Geissler lamp, since the central constriction (characteristic of the Geissler lamp) enhances greatly the brightness by increasing the current density, minimizes self-reversal, and produces light that can be very efficiently collected by a suitably-designed elliptical reflector and focused into a small volume. Its main differences from a commerically available Geissler lamp is that it has a heated cathode, has a central constriction of 5-mm bore, and is filled

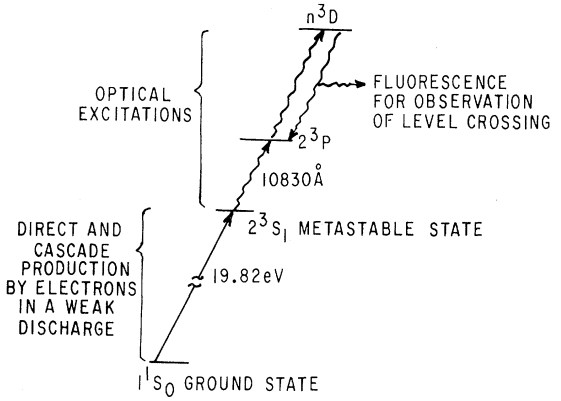

FIG. 4. Stepwise excitation scheme for the present experiment.

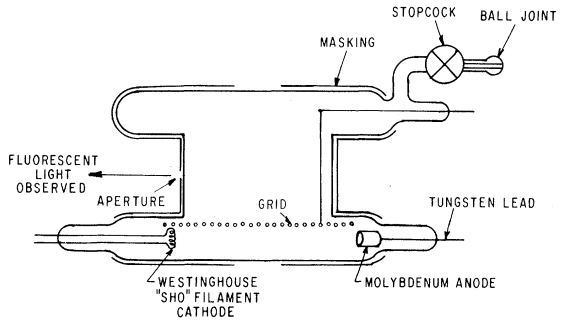

FIG. 5. Discharge-absorption cell.

at 2.3 torr for the best compromise for strong intensities in all the lines of interest. A lamp is typically run at 0.6-A dc at 135 V. Forced-air cooling is needed. Two lamps are used for the present experiment, each sitting at a line focus of an elliptical reflector, and the axis of the discharge-absorption cell sits at the common foci of the two elliptical reflectors. This bielliptical confocal system ensures excellent light collection from the lamps into the cell, allows multiple passes of light into the cell, and gives to the excitation light a good "directionality" (which is needed to produce a level-crossing signal). Typical photon fluxes (in cm^{-2} sec^{-1}) onto the center of the cell for the various lines of interest have been measured to be 8×10^{16} for 10 830Å; 2×10^{16} for 5876 Å; 3×10^{15} for 4472 Å; and 2×10^{15} for 3889 Å.

The complete setup is shown schematically in Fig. 6. Unpolarized light for excitation enters the cell in the y direction after passing through collimating Venetian blinds (to reduce instrumental scattering). The stepwise fluorescence is viewed within a small solid angle (opening angle ~5°) along the cell axis (the z direction), which is parallel to the direction of the sweeping magnetic field. The discharge in the cell is parallel to the z direction (so that the sweeping magnetic field

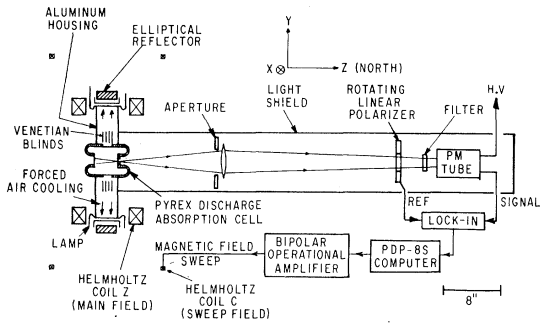

FIG. 6. Experimental setup.

does not significantly affect the discharge). Magnetic field in the x and y directions are bucked out by Helmholtz coils not shown in Fig. 6. The fluorescence is detected by an EMI 9558B photomultiplier after passing through appropriate interference filters. To observe a level crossing in a ^3D state, a rotating linear polarizer is used for lock-in detection, as shown in Fig. 6. However, to observe an "absorption level-crossing signal" (i.e., the effect of a crossing in $2\,^3P$ state on the stepwise fluorescence from a ^3D state), the rotating linear polarizer is removed, and a pair of "modulating coils" (not shown in Fig. 6) is used to produce a modulating z field for lock-in detection.

The calibration of the main coils Z (i.e., the gauss per ampere ratio averaged over the volume of observation) poses a problem initially, since the Z coils have a comparatively small radius (~8 in.) and a large cross section (~2.5×2.75 in.). The observation region is a roughly cylindrical volume about 0.5 in. in diameter (in the x-y plane) and 1.5 in. in length (in the z direction). The field inhomogeneity over this volume is found to be 6×10^{-4} of the mean field by NMR probing. As we are aiming at an accuracy of about 10^{-4} for our field determinations, it is important to get a suitably averaged calibration over the observation region. Fortunately, our present experimental setup is "self-calibrating," i.e., by observing certain fluorescence light from our setup itself, the calibration (automatically averaged over the observation region) can be found. In fact, this can be done in different ways, and at different fields (or different currents through the coils). First, conventional level-crossing signals and absorption level-crossing signals in the $2\,^3P$ and $3\,^3P$ states are easily observed in our setup; since the fine-structure intervals in these states have been precisely determined,[24,25] the positions of the level crossings can be calculated, and hence the field calibration can be deduced. Second, the metastable state in our setup is optically pumped, and we can readily do precision magnetometry by fluorescence monitoring.[26] The fact that the $2\,^3S$ metastable state in our setup is strongly pumped is manifested by the observed Hanle signal of the $3\,^3P$ state (Fig.7), which shows an extremely narrow peak at zero field due to ground-state level crossing.[27-29] This narrow peak also occurs in the stepwise fluorescence [Fig. 7(c)], which shows that the statement of Kibble *et al.*[22] that "level crossings in the initial term do not cause additional interferences" refers only to very weak excitation. From the above work we conclude that the calibration of the Z coils, averaged over the observation region, is constant at 14.440 ± 0.003 G/A (i.e., an uncertainty of $2/10^4$) from 0–400 G, after which it rises about linearly (probably due to thermal effects) to 14.443 ± 0.003 G/A at 600 G.

VI. DATA TAKING AND ANALYSIS

Data collection and control of the magnetic field sweep are done by a programmed PDP-8S minicomputer as indicated in Fig. 6. To observe a certain level-crossing signal, the mean field H_{av} is produced by the high-power Helmholtz coils Z. The sweeping of the field about H_{av} is provided by the low-power Helmholtz coils C controlled by the computer, i.e., the computer sweeps the current up and down in steps, and during each step the computer accumulates the signal. Each cycle takes about 2 min. After about 10 cycles, data accumulation is temporarily stopped, the magnetic field is reversed, and then the data accumulation is resumed, with the new data being accumulated on top of the old data. The same number of cycles as before is made. The process can be repeated till a satisfactory signal-to-noise ratio is obtained. The field-reversal procedure not only takes care of bias effects depending on direction of the field or the current (like a small component of the earth's field parallel to the z direction), but also eliminates the admixture of a small "dispersion" component in the Lorentzian level-crossing signal, as explained in the following. The phase of

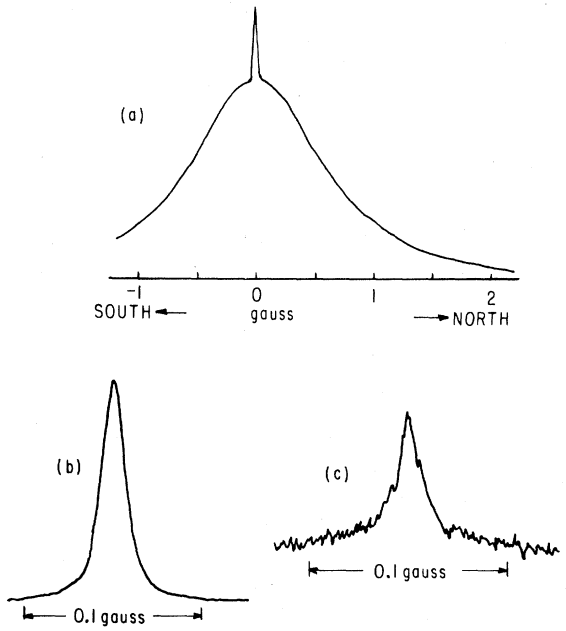

FIG. 7. (a) Chart recorder trace of the Hanle signal of the $3\,^3P$ state, observed by monitoring the $3\,^3P \rightarrow 2\,^3S$ fluorescence. (b) Blowup of the ground-state level-crossing signal in (a). (c) Ground-state level-crossing signal observed in the $3\,^3D \rightarrow 2\,^3P$ stepwise fluorescence.

TABLE II. Depolarization cross sections and critical pressures for $3\,^3D$ and $4\,^3D$.

$n\,^3D$	τ_0(nsec) Ref. 30	σ_{dep} (10^{-14}cm^2) High-field crossings Present work	Zero-field crossings Ref. 8	Zero-field crossings Ref. 31	P_c (mtorr) Present work
3	14.2	3.2±0.7	7	4.6±0.5	340
4	31.5	10±2	4	2.9±0.2	50

the lock-in amplifier (with respect to the rotating linear polarizer) has been set by symmetrizing a strong level-crossing signal (like the Q crossing of $3\,^3D$ state). This will automatically symmetrize all other level-crossing signals. However, we found that this phase setting for symmetrical signals varies slowly with time (to within ±5° from the initial setting). This may be due to various causes, e.g., slight changes in the spatial distribution of the excitation light. Hence, an unknown but small amount of (antisymmetrical) dispersion component always accompanies the (symmetrical) Lorentzian signal, which is an undesirable complication. Rose and Carovillano[20] have shown that the dispersion component has $\sin\beta$ as a factor, where β is the "phase angle misadjust" here, i.e., if the phase angle of the lock-in amplifier is changed by $-\beta$, the dispersion component would disappear. β is defined with respect to the field direction, and reverses sign when field direction reverses. Hence field-reversed dispersion components cancel on adding.

The center of each high-field level-crossing signal (except crossing S in $3\,^3D$, to be discussed later) is obtained by fitting it with a Lorentzian plus a possible sloping baseline. The possibility of a pressure dependence or a discharge-current dependence of the position of the center has been investigated. The normal helium pressure used is about 60 mtorr, and the normal discharge current in the absorption cell is about 20 mA. Signals have been observed at helium pressures up to 190 mtorr or discharge currents up to 45 mA, and no significant variations in the positions of the centers are found. However, we did find that the level-crossing widths increase very rapidly with pressure. By plotting the width versus pressure, the collisional-depolarization cross section σ_{dep} can be obtained. σ_{dep} is found to be approximately constant for P, Q, R, and S crossings in each state. We define the critical pressure P_c as the helium pressure when the crossing width is pressure broadened to twice the natural width, i.e.,

$$3.3\times10^{13}P_cV\sigma_{dep}\tau_0=1\,, \tag{22}$$

where P_c is the pressure in mtorr, V is the average relative velocity between two helium atoms, and τ_0 is the radiative lifetime. The present experimental σ_{dep} and related P_c are listed in Table II, where results from Hanle-effect experiments by ion-bombardment are also given. (The latter experiments are complicated by various cascade routes and by the very different "Hanle widths" for the $J=1,2,3$ states.)

To avoid too much pressure broadening of the level-crossing signals, the helium pressure should be kept below or at most comparable to P_c. However, discharge instabilities at pressure below 30 mtorr and also the rapid decrease in the metastable density as pressure decreases below about 50-mtorr force a compromise to be made for the experimental helium pressure, and the best com-

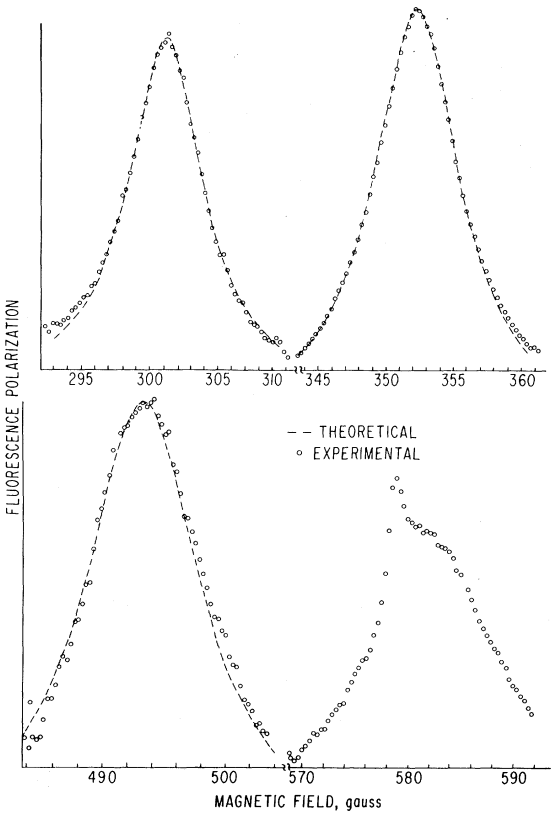

FIG. 8. Typical experimental signals for the high-field crossings in $3\,^3D$. (Broken line is the Lorentzian fit to the experimental data.)

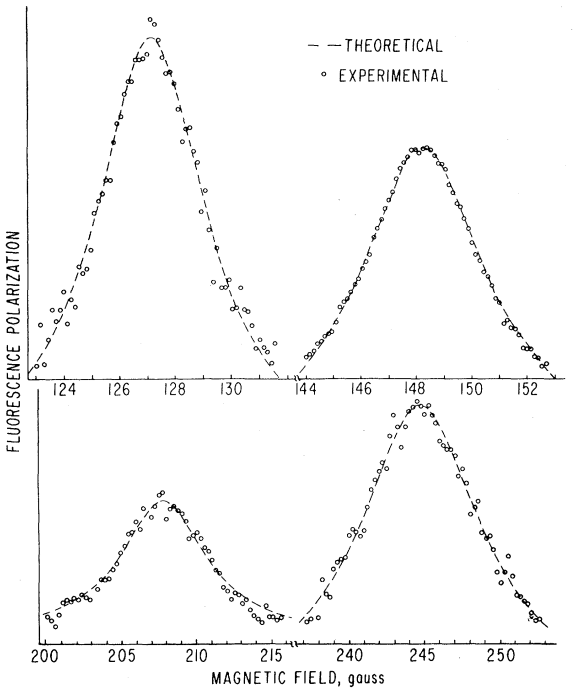

FIG. 9. Typical experimental signals for the high-field crossings in $4\,^3D$.

promise is found to be 30–80 mtorr for $3\,^3D$ and 30–60 mtorr for $4\,^3D$. Spectroscopy of any higher ^3D states would require lower-pressure ranges, and our present apparatus would not be very suitable.

Typical experimental signals for the P, Q, R, and S crossings in $3\,^3D$ and $4\,^3D$ are shown in Figs. 8 and 9, respectively. A typical integration time is about 1 h. The polarization observed at the center of a crossing as a percentage of the fluorescence is the following: 1% for crossing Q; 0.2% for crossing P; and 0.1% for crossings R and S. All the high-field crossing signals are fitted well by a Lorentzian except the S crossing in $3\,^3D$, where the occurrence of a multiplicative level crossing [i.e., the $2\,^3P$ crossing at 578.49 G overlaps with the $3\,^3D$ crossing at 582 G, which has a full width at half-maximum (FWHM) of about 14 G] results in a very extraordinary signal shape. This is the first instance of a multiplicative level-crossing signal at nonzero magnetic field. Unfortunately, no detailed analysis of this experimental signal has been made, because the overlapping of the multiplicative level-crossing signal with the conventional level-crossing signal results in a number of complications, which will be mentioned later in our discussion of the overlapping low-field level crossings.

The experimental level-crossing field, averaged over several runs, are listed in Table III for case A, when the uncertainty in the calibration of the Z coils is disregarded, so that the error quoted is purely statistical; and for case B, when the uncertainty in the calibration of the Z coils is included in the error stated. Since the uncertainty of two

TABLE III. Experimental level-crossing fields for $3\,^3D$ and $4\,^3D$ states and the corresponding fitted fine-structure intervals.

State	Point	Level crossing Field (G): Upper error is for case A and lower for case B [a]	Fitted fine-structure intervals; upper error for case A and lower for case B [a] $E_1 = {}^3D_1 - {}^3D_3$ (MHz)	$E_2 = {}^3D_2 - {}^3D_3$ (MHz)
$3\,^3D$	P	301.067 ± 0.023 ± 0.064		
	Q	352.172 ± 0.019 ± 0.073	1400.67 ± 0.05 ± 0.29	75.94 ± 0.23 ± 0.23
	R	493.239 ± 0.054 ± 0.112		
	S	582.25 ± 0.35 ± 0.37		
$4\,^3D$	P	127.156 ± 0.030 ± 0.039		
	Q	148.274 ± 0.026 ± 0.039	591.25 ± 0.07 ± 0.14	36.19 ± 0.27 ± 0.27
	R	207.84 ± 0.06 ± 0.07		
	S	244.68 ± 0.06 ± 0.08		

[a] In case A, the uncertainty in calibration of the Z coils is neglected, while in case B it is taken into account.

parts in 10^4 in the calibration of the Z coils tends to systematically shift all magnetic-field values by the same percentage in the same direction, it is more advantageous to extract the fine-structure intervals E_1 and E_2 from the experimental level-crossing fields for case A first, and then investigate the additional uncertainties in E_1 and E_2 when all crossing field values are increased by $2/10^4$ or decreased by $2/10^4$. The computer fitted E_1 and E_2 with uncertainties for these two cases (cases A and B) are also tabulated in Table III. This fitting is based on the mean values for the triplet coefficient α_t, orbital g value g_L, and spin g value g_S as given in Eqs. (21a)–(21c). The uncertainties in the fitted E_1 and E_2 values, resulting from the uncertainties in the parameters α_t, g_L, and g_S, are negligible as indicated in Table IV. However, should improvements on the present experiment enable accuracies of ±0.02 MHz for E_1 and ±0.04 MHz for E_2 to be achieved, then the effects of the uncertainties in α_t, g_L, and g_S would have to be considered. In other words, substantial improvements in accuracy over the present work would entail more careful examinations of the parameters α_t, g_L, and g_S for the ^3D states.

The over-all low-field level-crossing signal, i.e., the combination of crossings A, B, C, and D, has been observed for $3\,^3D$ and for $4\,^3D$ by the same method as for a high-field crossing, and a typical signal is shown in Fig. 10 for $3\,^3D$. A typical integration time is about 1 h. As the positions of the high-field crossings are mainly sensitive to the large fine-structure interval E_1, so are the positions of the low-field crossings mainly sensitive to the small fine-structure interval E_2. So the combined low-field signal should ideally give a much more accurate value for E_2 than that given in Table III. Unfortunately, complications due to the optical pumping of the $2\,^3S$ and the $2\,^3P$ states, the trapping of the 10 830-Å resonance radiation,

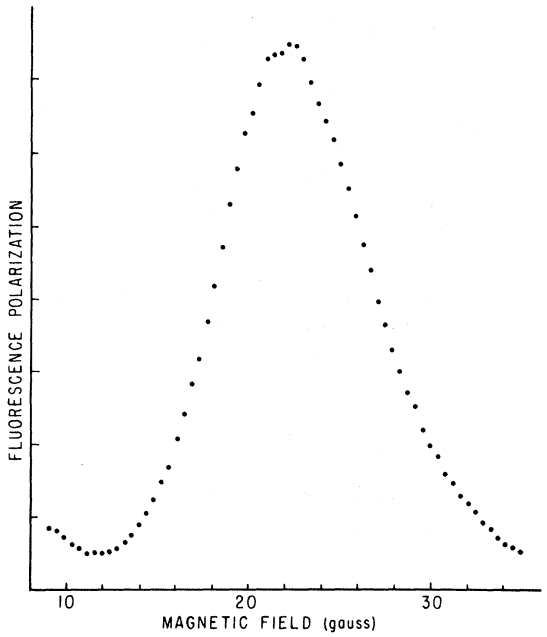

FIG. 10. Typical experimental signal for the overlapping low-field level crossings in $3\,^3D$.

and the opening angle (±25°) of the incident excitation light make accurate analysis of the over-all signal (consisting of four unresolved level-crossing signals) impossible. These difficulties arise only for the case of overlapping crossings, and have the effect of making uncertain the "weight" of each crossing. Also, at low fields, the "tails" of the zero-field crossings of the $^3D_1$, $^3D_2$ and $^3D_3$ states, all having quite different Hanle widths, are not negligible. Furthermore, the discharge in the discharge-absorption cell is rather diffused at low fields, and some "background variation" is superimposed on the rather wide combined level-crossing signal. Thus, detailed analysis based on Eq. (15) of the experimental lineshape was not made. Instead, a least-square fit for E_2 and the coherence lifetime τ is made by freely varying the weights of all crossings (A, B, C, D and the three zero-field crossings). The results thus obtained are shown in Table V.

TABLE IV. Effect of uncertainties in α_t, g_L, and g_S on the fitted values for the fine-structure intervals ($\bar{\alpha}_t = 0.999\,95$; $\bar{g}_L = 0.999\,867$; $\bar{g}_S = 2.002\,29$).

State	Deviation of one parameter from the mean value	Resultant deviation of fitted structure intervals from the mean value for E_1(MHz)	for E_2(MHz)
$3\,^3D$	$\alpha_t = \bar{\alpha}_t + 0.000\,05$	−0.005	−0.03
	$g_L = \bar{g}_L + 0.000\,01$	+0.008	−0.01
	$g_S = \bar{g}_S + 0.000\,04$	+0.014	+0.02
$4\,^3D$	$\alpha_t = \bar{\alpha}_t + 0.000\,05$	+0.001	+0.01
	$g_L = \bar{g}_L + 0.000\,01$	+0.002	−0.02
	$g_S = \bar{g}_S + 0.000\,04$	+0.008	+0.03

TABLE V. Results obtained from least-square fitting of the combined low-field level-crossing signal.

State	E_2(MHz)	τ(nsec) (at He pressure ≈ 50 mtorr)
$3\,^3D$	76.5 ± 1.0	12 ± 1
$4\,^3D$	36.0 ± 0.5	18 ± 2

TABLE VI. Testing of the n^{-3} scaling rule with the experimental fine-structure intervals of n^3D.

n	$n\,^3D_1 - n\,^3D_3 = E_1$ (MHz)	$n\,^3E_1$ (MHz)	$n\,^3D_2 - n\,^3D_3 = E_2$ (MHz)	$n\,^3E_2$ (MHz)
3 [a]	1400.67 ± 0.29	37 818 ± 8	75.97 ± 0.23	2056 ± 6
4 [a]	591.25 ± 0.14	37 840 ± 9	36.15 ± 0.24	2314 ± 15
5 [b]	302.3 ± 2	37 790 ± 250	20.3 ± 0.3	2538 ± 38
6 [b]	178 ± 3	38 400 ± 600	12.3 ± 0.3	2660 ± 60
7 [c]	99 ± 15	34 000 ± 5000	7.3 ± 0.3	2500 ± 100

[a] Present work.
[b] Dily and Descoubes, Ref. 6.
[c] Berry *et al.*, Ref. 9.

VII. SUMMARY AND DISCUSSIONS

The fine-structure intervals of the lowest two triplet D states of helium are determined, and are listed in Table I (values of E_2 given in Tables III and V have been combined). Results from all previous measurements and from calculations are also given.

From Table I, we see that our present experimental results are much more accurate than the others, and are consistent with them except in the case of $3\,^3D_2$-$3\,^3D_3$, where our value of 75.97 ± 0.23 MHz disagrees with Descoubes's value of 72.5 ± 0.5 MHz obtained by electron-bombardment level-crossing spectroscopy. We believe that the latter value is in error, possibly due to systematic errors not entirely accounted for.

It seems obvious from Table I that agreement between experiment and theory is poor, especially for the $^3D_2$-$^3D_3$ interval. Clearly, more refined theories are needed to understand better theoretically the fine structures and singlet-triplet mixing in the triplet D states of helium.

Finally, we can check whether the triplet D fine structures satisfy the n^{-3} scaling rule predicted by the simple theory of Bethe and Salpeter[12] (which neglect singlet-triplet mixing among other things). From Table VI, we see that E_1 (which is independent of singlet-triplet mixing) fits an n^{-3} scaling remarkably well, and we can probably put

$$n^3E_1 = 37\,830 \pm 300 \text{ MHz} \tag{23}$$

to obtain better values of E_1 at $n \geq 6$. However, we see that E_2 (which is quite sensitive to the degree of singlet-triplet mixing, and is smaller when mixing is stronger) deviates very significantly from an n^{-3} scaling law, and the deviation (in the negative direction) is more serious as n decreases to 3. This could be compared to the theoretical finding[1,2] that mixing increases rapidly as n decreases to 3.

ACKNOWLEDGMENTS

The author is indebted to Professor William Happer and to Dr. Henry Y. S. Tang for advise, encouragement, and support.

†This work was supported in part by the Joint Services Electronics Program (U.S. Army, U.S. Navy, and U.S. Air Force) under Contract DAAB07-74-C-0341, and in part by the Air Force Office of Scientific Research under Grant AFOSR-74-2685.

[1] R. K. Van den Eynde, G. Wiebes, and Th. Niemeyer, Physica 59, 401 (1972).
[2] R. M. Parish and R. W. Mires, Phys. Rev. A 4, 2145 (1971).
[3] D. Krause and E. A. Soltysik, Phys. Rev. A 6, 694 (1972).
[4] R. B. Kay and R. H. Hughes, Phys. Rev. 154, 61 (1967); R. B. Kay and J. G. Showalter, Phys. Rev. A 3, 1998 (1971).
[5] J. Brochard, R. Chabbal, H. Chantrel, and P. Jacquinot, J. Phys. Radium 18, 596 (1957).
[6] J. P. Descoubes, in *Physics of the One- and Two-Electron Atoms*, edited by F. Bopp and H. Kleinpoppen (North-Holland, Amsterdam, 1969), p. 341; D. Dily and J. P. Descoubes, C. R. Acad. Sci. (Paris) B 272, 1182 (1971); and J. P. Descoubes, thesis (Univ. de Paris, 1967) (unpublished).
[7] R. D. Kaul, J. Opt. Soc. Am. 58, 429 (1968).
[8] K. Buchhaupt, Z. Naturforsch. 24a, 1058 (1969).
[9] H. G. Berry, J. L. Subtil, and M. Carre, J. Phys. (Paris) 33, 947 (1972).
[10] T. A. Miller and R. S. Freund, Phys. Rev. A 5, 588 (1972).
[11] W. Wittmann, K. Tillmann, H. J. Andra, and P. Dobberstein, Z. Phys. 257, 279 (1972).
[12] H. A. Bethe and E. E. Salpeter, *Handbuch der Physik* (Springer-Verlag, Berlin, 1957), Vol. 35, p. 88.
[13] G. Araki, M. Ohta, and K. Mano, Phys. Rev. 116, 651 (1959).
[14] G. W. F. Drake, Phys. Rev. 181, 23 (1969).
[15] A. F. J. Van Raan and H. G. M. Heideman, J. Phys.

B 7, L216 (1974); A. F. J. Van Raan, P. G. Moll, and J. van Eck, *ibid.* 7, 950 (1974).
[16]G. Araki, Proc. Phys. Math. Soc. Jpn. 19, 128 (1937).
[17]N. Bessis, H. Lefebvre-Brion, and C. M. Moser, Phys. Rev. 135, A957 (1964); and C. Ambry, N. Bessis, and C. M. Moser, Phys. Rev. 170, 131 (1968).
[18]F. D. Colegrove, P. A. Franken, R. R. Lewis, and R. H. Sands, Phys. Rev. Lett. 3, 420 (1959).
[19]P. A. Franken, Phys. Rev. 121, 508 (1961).
[20]M. E. Rose and R. L. Carovillano, Phys. Rev. 122, 1185 (1961).
[21]W. Happer, in *Beam Foil Spectroscopy,* edited by S. Bashkin (Gordon and Breach, New York, 1968), p. 305.
[22]B. P. Kibble and S. Pancharatnam, Proc. Phys. Soc. Lond. 86, 1351 (1965).
[23]R. Gupta, S. Chang, and W. Happer, Phys. Rev. A 6, 529 (1972).
[24]S. A. Lewis, F. M. J. Pichanick, and V. W. Hughes, Phys. Rev. A 2, 86 (1970); and A. Kponou, V. W. Hughes, C. E. Johnson, S. A. Lewis, and F. M. J. Pichanick, Phys. Rev. Lett. 26, 1613 (1971).
[25]I. Wieder and W. E. Lamb, Phys. Rev. 107, 125 (1957).
[26]L. D. Schearer and F. D. Sinclair, Phys. Rev. 175, 36 (1968).
[27]R. W. Schmieder, A. Lurio, W. Happer, and A. Khadjavi, Phys. Rev. A 2, 1216 (1970).
[28]A. Kastler, Nucl. Instrum. Methods 110, 259 (1973).
[29]R. E. Slocum, Phys. Rev. Lett. 29, 1642 (1972).
[30]W. L. Wiese, M. W. Smith, and B. M. Glennon, *Atomic Transition Probabilities* (U. S. GPO, Washington, D. C., 1966), Vol. I.
[31]K. Buchhaupt, Z. Naturforsch. 27a, 572 (1972).
[32]T. A. Miller, R. S. Freund, and B. R. Zegarski, Phys. Rev. A 11, 753 (1975).